

April 2, 2016

Dear Editor.

We thank the reviewers for their time and suggestions. Attached please find our answers to the specific comments raised by the reviewers and some extra figures and supplementary table we have added. **Our replies are in bold**

□Our replies

Reviewer 1

1.Line 128: I think you mean microM, rather than micromol.

Yes, changed

2.Line 134-135: describe briefly here the rationale for the delineation of the P1 and P2 time periods. I know they are described in other parts of this special issue, but if someone were to read only this paper, it would be good to describe why this choice was made here.

The chemical and biological changes that occurred in each of the experimental stages are described in detail at the beginning of the results section. Section 3.1). We have, however, added the following sentences at end of section 2.1 to clarify the rationale of these delineations.

“Based on the results of different biogeochemical and biological parameters during VAHINE (Turk-Kubo et al., 2015; Berthelot et al., 2015; Bonnet et al.,), three specific periods were discerned (see detailed description in section 3.1) within which we have also investigated TEP dynamics: Days 2-4 (P0) are the pre-fertilization days when the DIP concentrations were 0.02-0.05 PO_4^{3-} and combined DIN were extremely low; days 5-14 (P1) –After fertilization on day 5 the PO_4^{3-} concentrations were $\sim 0.8 \mu\text{mol L}^{-1}$ and diazotrophic populations were dominated by diatom-diazotroph associations. The second stage of the experiment (P2) from days 15 to 23 was characterized by simultaneous increase in primary and bacterial production as well as in N_2 fixation rates which averaged $27.7 \text{ nmol L}^{-1} \text{ d}^{-1}$ (Berthelot et al. 2015) and diazotrophic populations comprised primarily by the unicellular UCYN-C (Turk-kubo et al 2015).”

3.Line 230: close parentheses around *Synechococcus*

parentheses added

4.Line 274-277: I think the reader would benefit from a slightly different description of the trends seen in the first days. Upon my first reading, I only imagined the spike that occurred after the phosphate addition, but the TEP was increasing during the entire P0 phase, spiked in the hours after phosphate addition, then decreased during P1

Line 274-277: TEP concentrations increased from the lowest volumetric concentrations (averaging $\sim 50 \mu\text{g GX L}^{-1}$) measured on day 2 to reach maximum concentrations in each of the mesocosms (average of $\sim 800 \mu\text{g GX L}^{-1}$) on day 5, ~ 15 h after the mesocosms were fertilized with DIP (Fig. S1, Fig. 1a).

5.Line 284-285: the sections seem to be mixed up here. Do you mean that the lagoon increased in TEP during P0 and P2, but decreased during P1?

Yes, there was a mistake in the sentence. Fixed to:

“TEP concentrations in the lagoon water were compared with those in the mesocosms. These showed a similar pattern of increase in TEP during P0 and P2 while the gradual decline in TEP concentrations during P1 was not statistically significant as observed in the mesocosms (Fig. 1, Fig. S1).”(there is no P3 it’s a mistake- deleted and change in text)

6.Line 350-351: DIP turnover rates indicate DIP stress or deficiency. That cannot fully indicate limitation without some sort of calibration.

You are right. Turnover rates alone do not indicate deficiency. However, increasing Alkaline phosphatase activity (APA) in M1 and M2 from day 18 and in M3 from day 21 suggests that the cells were responding to P stress (Van Wambeke et al. this issue). We have rephrased the sentence

7. Line 467: I suspect the organic matrix around the UCYN-C was EPS produced by and remaining close to the cells (similar to what some phenotypes of UCYN-B do), rather than material that was released and then aggregated free-living cells of UCYN-C. I know it’s a small distinction, and perhaps meaningless to many, but I also think it’s worth noting that this is a possible scenario and there is precedent to believe that is what happened.

We agree with you as to the mechanism of aggregation. We have modified the sentence making this distinction

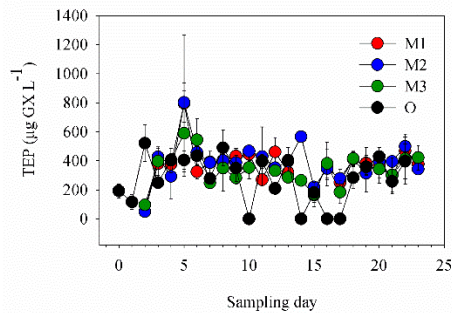
“Furthermore, UCYN-C probably produced an organic matrix possibly also comprised of TEP that aided the formation of large aggregates (100-500 μm) (Fig. 6g-h). These aggregates were predominantly responsible for the enhanced export production ($22.4 \pm 5\%$ of exported POC), (Knapp et al., 2015; Bonnet et al., 2016 – both in this special issue-.”

8.Lines 473-490: was this Trichodesmium bloom at the lagoon control sampling site, or elsewhere in the lagoon? Does it explain any of the results from the experiment or the lagoon results? If not, I don’t really think it belongs here, as it is a description of a non-related phenomenon.

Yes, Trichodesmium bloomed at the lagoon control sampling site. However, upon rereading the paragraph and your comment, we agree that it does not provide any further explanation of the results and have thus removed the whole paragraph.

Paper Figure 1: I would like to see all the figures put on the same X axis to make them more directly comparable. I know it will be harder to see patterns, but the comparison is more important, I think

All plots of Fig 1 are on the same X axis. We have now presented them with the same Y scale. We here include a supplemental figure with the average TEP concentration from each mesocosm and from the lagoon on the same plot to easily compare. These show how uniform overall TEP content is but when dissected each mesocosm shows a similar pattern of increase and decrease that we want to emphasize.



Reviewer 2

- Looking at Fig.1, it seems that the only major difference between the mesocosms and the surrounding water is the spike in TEP concentration inside mesocosms immediately after the P addition. The other trends seem to be similar. Any idea why?

This has been described in section 3.1.1 . The difference between the TEP in the mesocosms and the lagoon water is hard to see and is significantly different immediately after P addition and only during P1 after P addition and subsequent utilization when declining P availability was correlated with increased TEP concentrations. The decline in TEP concentrations from the lagoon water during P1 was not statistically significant as demonstrated in the mesocosms (Fig. 1, Fig. S1). The significant decline in TEP in the first days after P addition is probably due to two factors: a) phytoplankton relieved of P stress will produce less TEP and increase growth rates, b) bacteria will utilize the added P as well as TEP and other organic C sources to grow – so higher TEP consumption and therefore a more significant decline in the mesos compared to the lagoon.

- Did the authors check whether the optical absorption method using the Alcian blue dye staining to determine TEP concentration is linear? Was the filter absorption measured using the integrating sphere? If not, was there any significant scattering?

TEP concentrations are determined from an Alceline blue (AB) calibration curve done. AB was calibrated using different volumes of purified polysaccharide GX and - The absorption measured was done with a spectrophotometer (Cary 100) equipped with an integrated sphere.

- Do the authors have control data from the lagoon outside the mesocosms to be added into Figs.3-6?

Control data for figures 3-5 are available in supplementary figures we show here (below). As none of them had any significant correlation we decided not to show them but only state this in the text.

For Fig 6 no data exists of DDA growth rates in the lagoon (control) water. We have also added all the statistics we performed for the control (out) versus the parameters tested for the mesocosms in the revised supplementary Table S2 (attached here)

- Any idea why was TOC significantly higher in M3? Why TEP did not increase proportionally?

M3 had higher biomass both PP and bacterial which enriched TOC (Berthelot et al. 2015) and a full discussion on the replicability and variability of the mesocosms can be found in the introductory paper to the project (Bonnet et al. 2016) . Why TEP did not increase proportionally is a good question – although when we look at fig 5 we can see a similar slope of BP to TEP concentration but shifted to higher production levels of BP that were found in M3. The higher BP possibly indicates a greater extent of utilization of TEP and organic C so that the resulting concentrations which we measured did not significantly change.

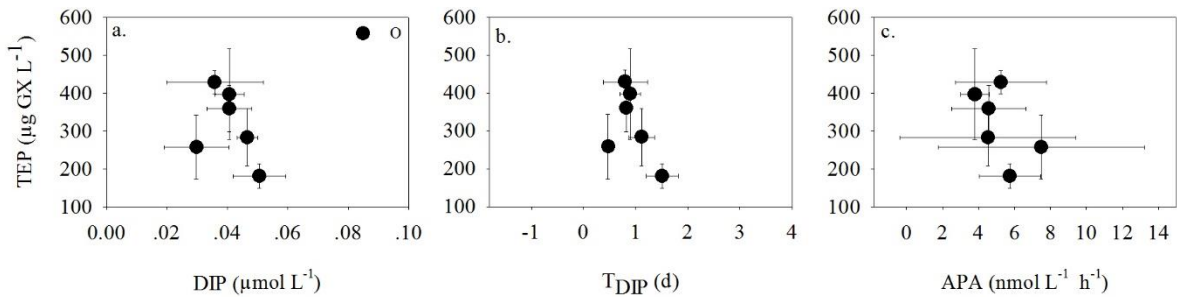


Figure 3S – relationship between TEP concentrations to DIP, TDIP, and APA activity measured in the lagoon throughout the VAHINE experiment.

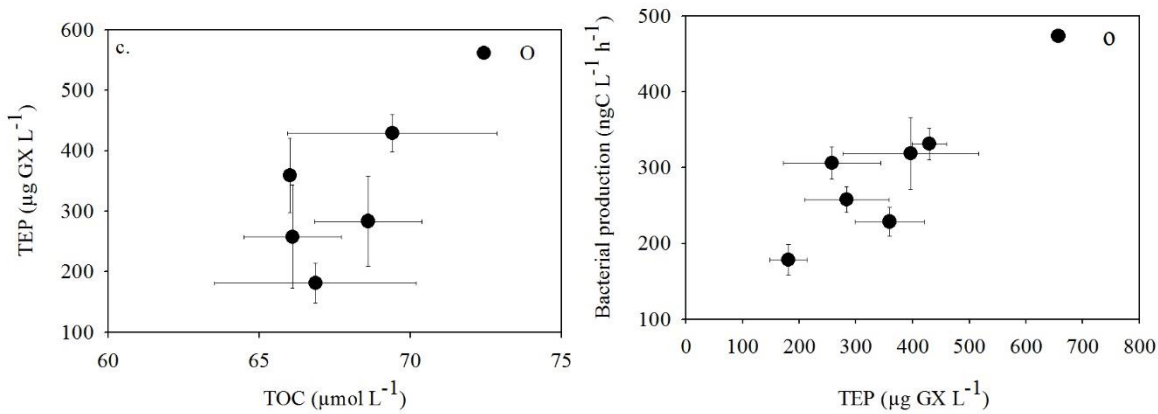


Figure 4S. Relationship between TEP concentrations measured in the Lagoon (outside the mesocosms) to concentrations of total organic carbon (TOC) and bacterial production measured throughout the VAHINE experiment.

Table S2. Pearson's linear regression analyses between the average concentration of transparent exopolymeric particles [TEP ($\mu\text{g GX L}^{-1}$)] and the physical, chemical, and biological parameters from each mesocosm (M1, M2, M3) and outside waters (O) divided into the two postfertilization phases of the VAHINE experiment. P1 = days 5-14, P2 = days 15-23. Each TEP value is an average of the measurements from three sampled depths. Correlations in bold are statistically significant with $P < 0.05$. For Het-1 and UCYN-C the growth rate (μ) is the net growth rate, based on changes of nifH copies L^{-1} from day to day.

Parameter	Mesocosm	Period	R2	P	n	
Temperature (°C)	M1	P1	0.055	0.577	8	
	M2		0.015	0.776	8	
	M3		0.191	0.279	8	
	O	P2	0.156	0.381	7	
	M1		0.369	0.148	7	
	M2		0.087	0.520	7	
	M3		0.357	0.157	7	
	O		0.001	0.955	5	
	DIP ($\mu\text{mol L}^{-1}$)	M1	P1	0.011	0.805	8
		M2		0.055	0.544	9
M3		0.295		0.163	8	
O		P2	0.038	0.677	7	
M1			0.031	0.676	8	
M2			0.539	0.038	8	
M3			0.249	0.123	8	
O			0.171	0.415	6	
DOP ($\mu\text{mol L}^{-1}$)		M1	P1	0.000	0.965	8
		M2		0.198	0.229	9
	M3	0.004		0.879	8	
	O	P2	0.042	0.658	7	
	M1		0.128	0.383	8	
	M2		0.367	0.112	8	
	M3		0.141	0.320	9	
	O		0.705	0.075	5	
	POP ($\mu\text{mol L}^{-1}$)	M1	P1	0.020	0.738	8
		M2		0.050	0.563	9
M3		0.039		0.641	8	
O		P2	0.145	0.399	7	
M1			0.103	0.401	9	
M2			0.005	0.851	9	
M3			0.192	0.237	9	
O			0.0005	0.968	6	

	M1		0.077	0.51	8
	M2	P1	0.012	0.775	9
	M3		0.043	0.620	8
T _{DIP} (d)	O		0.073	0.557	7
	M1		0.238	0.182	9
	M2	P2	0.523	0.028	9
	M3		0.338	0.100	9
	O		0.239	0.325	6
	M1		0.155	0.294	9
	M2	P1	0.432	0.077	8
	M3		0.048	0.638	7
APA	O		0.075	0.553	7
(nmole L ⁻¹ h ⁻¹)	M1		0.173	0.265	9
	M2	P2	0.683	0.011	8
	M3		0.300	0.126	9
	O		0.281	0.280	6
	M1		0.005	0.879	7
	M2	P1	0.003	0.882	9
	M3		0.051	0.591	8
DOC	O		0.036	0.686	7
(μmol L ⁻¹)	M1		0.266	0.295	6
	M2	P2	0.268	0.482	4
	M3		0.285	0.275	6
	O		0.008	0.888	5
	M1		0.213	0.211	9
	M2	P1	0.005	0.853	9
	M3		0.216	0.246	8
POC	O		0.099	0.493	7
(μmol L ⁻¹)	M1		0.006	0.883	6
	M2	P2	0.212	0.358	6
	M3		0.911	0.046	4
	O		0.014	0.883	4
	M1		0.105	0.434	8
TOC	M2	P1	0.003	0.883	9
(μmol L ⁻¹)	M3		0.002	0.926	8
	O		0.006	0.869	7

	M1		0.745	0.012	7
	M2	P2	0.728	0.007	8
	M3		0.582	0.046	7
	O		0.222	0.422	5
	M1		0.112	0.417	8
	M2	P1	0.042	0.597	9
	M3		0.041	0.632	8
DON	O		0.037	0.677	7
($\mu\text{mol L}^{-1}$)	M1		0.166	0.316	8
	M2	P2	0.718	0.008	8
	M3		0.379	0.104	8
	O		0.061	0.638	6
	M1		0.381	0.103	8
	M2	P1	0.160	0.286	9
	M3		0.334	0.133	8
PON	O		0.084	0.527	7
($\mu\text{mol L}^{-1}$)	M1		0.000	0.990	6
	M2	P2	0.330	0.233	6
	M3		0.036	0.720	6
	O		0.232	0.519	4
	M1		0.041	0.629	8
	M2	P1	0.325	0.140	8
	M3		0.007	0.858	7
N ₂ fixation	O		0.0002	0.980	6
($\text{nmol L}^{-1} \text{d}^{-1}$)	M1		0.046	0.579	9
	M2	P2	0.038	0.617	9
	M3		0.405	0.065	9
	O		0.267	0.293	6
	M1		0.251	0.169	9
	M2	P1	0.080	0.460	9
	M3		0.054	0.581	8
Chlorophyll a	O		0.056	0.609	7
($\mu\text{g L}^{-1}$)	M1		0.096	0.418	9
	M2	P2	0.126	0.348	9
	M3		0.292	0.133	9
	O		0.057	0.649	6

	M1		0.078	0.504	8
	M2		0.046	0.577	9
	M3	P1	0.209	0.254	8
PP	O		0.029	0.713	7
($\mu\text{mol C L}^{-1} \text{d}^{-1}$)	M1		0.000	0.991	8
	M2		0.332	0.105	9
	M3	P2	0.124	0.392	8
	O		0.499	0.117	6
	M1		0.083	0.488	8
	M2		0.000	0.973	9
	M3	P1	0.549	0.035	8
BB	O		0.266	0.236	7
($\text{ngC L}^{-1} \text{h}^{-1}$)	M1		0.574	0.029	8
	M2		0.424	0.058	9
	M3	P2	0.567	0.031	8
	O		0.153	0.444	6
	M1	P1	0.767	0.124	4
	M2		0.999	0.021	3
	M3		N.A	N.A	N.A
Het1	O		-	-	-
(μ)	M1	P2	0.837	0.029	5
	M2		0.754	0.132	4
	M3		0.137	0.540	5
	O		-	-	-
	M1	P1	N.A	N.A	N.A
	M2		0.005	0.953	3
	M3		N.A	N.A	N.A
UCYN-C	O		-	-	-
(μ)	M1	P2	0.421	0.236	5
	M2		0.694	0.167	4
	M3		0.775	0.049	5
	O		-	-	-

DIP: dissolved inorganic *phosphate*; DOP and POP: dissolved and particulate organic *phosphate*; T_{DIP} : Turnover rates of dissolved inorganic phosphate; APA: Alkaline phosphatase activity; DOC and POC: dissolved and particulate organic carbon; TOC: total organic carbon; DON and PON: dissolved and particulate organic nitrogen; BP and PP- bacterial and primary production.

1 **Dynamics of transparent exopolymer particles (TEP) during**
2 **the VAHINE mesocosm experiment in the New Caledonia**
3 **lagoon**

4
5 **I. Berman-Frank¹, D. Spungin¹, E. Rahav^{1,2}, F. Van Wambeke³, K. Turk-Kubo⁴, T.**
6 **Moutin³**

7 [1] Mina and Everard Goodman Faculty of Life Sciences, Bar-Ilan University, Ramat Gan,
8 Israel 5290002

9 [2] National Institute of Oceanography, Israel Oceanographic and Limnological Research,
10 Haifa, Israel

11 [3] Aix Marseille Université, CNRS/INSU, Université de Toulon, IRD, Mediterranean
12 Institute of Oceanography (MIO) UM110, 13288, Marseille, France

13 [4] Ocean Sciences Department, University of California, Santa Cruz, 1156 High Street, Santa
14 Cruz, CA, 95064, USA

15
16 Correspondence to: I. Berman-Frank (ilana.berman-frank@biu.ac.il)

27 **Abstract**

28 In the marine environment, transparent exopolymeric particles (TEP) produced from abiotic
29 and biotic sources link the particulate and dissolved carbon pools and are essential vectors
30 enhancing vertical carbon flux. We characterized spatial and temporal dynamics of TEP
31 during the VAHINE experiment that investigated the fate of diazotroph derived nitrogen and
32 carbon in three, replicate, dissolved inorganic phosphorus (DIP)-fertilized 50 m³ enclosures in
33 an oligotrophic New Caledonian lagoon. During the 23 days of the experiment, we did not
34 observe any depth dependent changes in TEP concentrations in the three sampled-depths (1,
35 6, 12 m). TEP carbon (TEP-C) content per mesocosm averaged $28.9 \pm 9.3\%$ and $27.0 \pm 7.2\%$
36 of TOC in the mesocosms and surrounding lagoon respectively and was strongly and
37 positively coupled with TOC during P2. TEP concentrations declined for the first 9 days after
38 DIP fertilization (P1 = days 5-14) and then gradually increased during the second phase (P2 =
39 days 15-23). Temporal changes in TEP concentrations paralleled the growth and mortality
40 rates of the diatom-diazotroph association of *Rhizosolenia* and *Richelia* that predominated the
41 diazotroph community during P1. By P2, increasing total primary and heterotrophic bacterial
42 production consumed the supplemented P and reduced availability of DIP. For this period,
43 TEP concentrations were negatively correlated with DIP availability and turnover time of DIP
44 (T_{DIP}) while positively associated with enhanced alkaline phosphatase activity (APA) that
45 occurs when the microbial populations are P-stressed. During P2, increasing bacterial
46 production (BP) was positively correlated with higher TEP concentrations which were also
47 coupled with the increased growth rates and aggregation of the unicellular UCYN-C
48 diazotrophs which bloomed during this period. We conclude that the composite processes
49 responsible for the formation and breakdown of TEP yielded a relatively stable TEP pool
50 available as both a carbon source and facilitating aggregation and flux throughout the
51 experiment. TEP was probably mostly influenced by abiotic physical processes during P1
52 while biological activity (BP, diazotrophic growth and aggregation, export production) mainly
53 impacted TEP concentrations during P2 when DIP-availability was limited.

54

55 **1 Introduction**

56 The cycling of carbon (C) in the oceans is a complex interplay between physical,
57 chemical, and biological processes that regulate the input and the fate of carbon within the
58 ocean. An essential process driving the flux of carbon and other organic matter to depth and
59 enabling long term sequestration and removal of carbon from the atmosphere is the biological

60 pump that drives organic C formed during photosynthesis to the deep ocean. This process,
61 termed export production (Eppley and Peterson, 1979), is facilitated via physical inputs of
62 ‘new’ nutrients (e.g. nitrogen, phosphorus, silica, trace metals, etc.) into the euphotic zone
63 from either external sources (deep mixing of upwelled water, river discharge, dust deposition,
64 and anthropogenic inputs) or via biological processes such as microbial N₂ fixation that
65 converts biologically unavailable dinitrogen (N₂) gas into bioavailable forms of nitrogen and
66 enhances the productivity of oligotrophic oceanic surface waters that are often limited by
67 nitrogen (Falkowski, 1997; Capone, 2001).

68 Marine N₂ fixation is performed by diverse prokaryotic organisms comprised
69 predominantly of autotrophic cyanobacteria and heterotrophic bacteria (Zehr and Kudela,
70 2011). To supply the energetically-expensive process of converting N₂ to ammonia (Stam et
71 al., 1987; Postgate and Eady, 1988; Mulholland and Capone, 2000), these organisms must
72 obtain energy from either photosynthesis (cyanobacteria) or from bioavailable organic carbon
73 compounds within the aquatic milieu (heterotrophic bacteria and mixotrophs). The total
74 organic carbon (TOC) in the ocean contains dynamic particulate (POC) and dissolved organic
75 carbon (DOC) pools that are supplied by biotic sources that are broken down into organic C-
76 containing marine microgels which include transparent polymeric particles (TEP). TEP are
77 predominantly acidic polysacchridic organic particles ranging in size from ~0.45 to > 300 μm
78 and are found in both marine and freshwater habitats (Passow, 2002). Both biotic and abiotic
79 processes form aquatic TEP that are routinely detected by staining with Alcian Blue
80 (Alldredge et al., 1993; Passow and Alldredge, 1995). Abiotic TEP occur by coagulation of
81 colloidal precursors in the pool of dissolved organic matter (DOM) and from planktonic
82 debris (Passow, 2002; Verdugo and Santschi, 2010) that may be stimulated by turbulence or
83 by bubble adsorption (Logan et al., 1995; Zhou et al., 1998; Passow, 2002). Biotically TEP
84 form from extracellular excretion or mucilage in algae and bacteria and from grazing and
85 microbial breakdown of larger marine snow particles [reviewd in (Passow, 2002; Bar-Zeev et
86 al., 2015)].

87 TEPs are light and bouyant (Azetsu-Scott and Passow, 2004). Yet, once formed, TEPs
88 sticky nature enhances and consolidates the formation of larger aggregates such as
89 marine/lake snow providing favorable environments for diverse microorganisms (Passow,
90 2002; Engel, 2004). Sedimentation of TEP associated “hot spots” from the surface are
91 important for transporting particulate organic material and microorganisms to deeper waters
92 (Smith and Azam, 1992; Azam and Malfatti, 2007; Bar-Zeev et al., 2009). During

93 sedimentation, TEP can also function as a direct source of carbon and other nutrients for
94 higher trophic level organisms such as protists, micro-zooplankton, and nekton (Passow,
95 2002; Engel, 2004).

96 TEP production can be enhanced in late phases of algal blooms and in senescent or
97 nutrient-stressed phytoplankton (Grossart et al., 1997; Passow, 2002; Engel, 2004;
98 Berman-Frank et al., 2007). Thus, TEP in oligotrophic waters (Engel, 2004) provide a source
99 of available carbon to fuel microbial food webs (Azam and Malfatti, 2007) that typically
100 succeed autotrophic blooms. TEP based aggregates or marine snow containing TEP typically
101 with high carbon (C): nitrogen (N) ratios (Wood and Van Valen, 1990; Berman-Frank and
102 Dubinsky, 1999), which can also fuel N₂ fixation by heterotrophic diazotrophs both in
103 oxygenated surface waters and in the aphotic zones (Rahav et al., 2013; Benavides et al., in
104 press).

105 The VAHINE project was designed to examine the fate/s of 'newly'-fixed N by
106 diazotrophs or diazotroph-derived N (hereafter called DDN) in the pelagic food web using
107 large mesocosms in the oligotrophic tropical lagoon of New Caledonia where diverse
108 diazotrophic populations have been observed (Dupouy et al., 2000; Garcia et al., 2007; Rodier
109 and Le Borgne, 2008; Biegala and Raimbault, 2008; Rodier and Le Borgne, 2010; Bonnet et
110 al., This issue-b). One of the major questions addressed during VAHINE was whether
111 diazotroph blooms significantly modify the stocks, fluxes, and ratios of biogenic elements (C,
112 N, P, Si) and the efficiency of carbon export. To this end, the 3 large-volume (~50 m³)
113 mesocosms containing ambient lagoon waters were fertilized with 0.8 μM DIP, and multiple
114 parameters were measured inside and outside of the mesocosms for 23 days (details of
115 parameters and experimental setup in (Bonnet et al., This issue-b). Within the VAHINE
116 framework, our specific objectives were: 1) to examine the spatial and temporal dynamics of
117 TEP; 2) to determine whether TEP content was regulated by nutrient status in the mesocosms
118 - specifically DIP availability; 3) to examine the relationship between TEP content, particulate
119 and dissolved carbon, and primary or heterotrophic bacterial production; and 4) to elucidate
120 whether TEP provided a source of energy for diazotrophs/bacteria/mixotrophs in mesocosms.

121

122 **2 Methods**

123 **2.1 Study site, mesocosm description, and sampling strategy**

124 Three large-volume (~50 m³) mesocosms were deployed at the exit of the oligotrophic
125 New Caledonian lagoon (22°29.10 S–166°26.90 E), from 13 January 2013 (day 1) to 4

126 February 2013 (day 23). The complete description of the mesocosm design and deployment,
127 as well as sampling strategy is detailed in Bonnet et al. (This issue-b). The mesocosms were
128 intentionally supplemented with $0.8 \mu\text{mol} \mu\text{Mmol L}^{-1}$ KH_2PO_4 (hereafter referred to as DIP
129 fertilization) between day 4 and 5 day of the experiment to promote N_2 fixation. Samples
130 were collected during the early morning of each day for 23 days with a clean Teflon pumping
131 system from 3 selected depths (1 m, 6 m, 12 m) in each mesocosm (M1, M2 and M3) and
132 outside (hereafter called 'lagoon waters'-O). Based on the results of different biogeochemical
133 and biological parameters during VAHINE (Turk-Kubo et al., 2015; Berthelot et al., 2015;
134 Bonnet et al., ~~This issue-a~~), three specific periods were discerned (see detailed description in
135 section 3.1) within which we have also investigated TEP dynamics: Days 2-4 (P0) are the pre-
136 fertilization days when the DIP concentrations were 0.02-0.05 PO_4^{3-} and combined DIN were
137 extremely low; days 5-14 (P1) After fertilization on day 5 the PO_4^{3-} concentrations were
138 $\sim 0.8 \mu\text{mol L}^{-1}$ and diazotrophic populations were dominated by diatom-diazotroph
139 associations. The second stage of the experiment (P2) from, and days 15- to 23 (P2) was
140 characterized by simultaneous increase in primary and bacterial production as well as in N_2
141 fixation rates which averaged $27.7 \text{ nmol L}^{-1} \text{ d}^{-1}$ (Berthelot et al. 2015) and diazotrophic
142 populations comprised primarily by the unicellular UCYN-C (Turk-kubo et al 2015).

Formatted: Superscript

Formatted: Subscript

Formatted: Superscript

Formatted: Subscript

Formatted: Superscript

Formatted: Superscript

143 2.2 TEP quantification

144 Water samples (100 mL) were gently (< 150 mbar) filtered through a $0.45 \mu\text{m}$
145 polycarbonate filters (GE Water & Process Technologies). Filters were then stained with a
146 solution of 0.02% Alcian Blue (AB) and 0.06% acetic acid (pH of 2.5). The excess dye was
147 removed by a quick deionized water rinse. Filters were then immersed in sulfuric acid (80%)
148 for 2 h, and the absorbance at 787 nm was measured spectrophotometrically (CARY 100,
149 Varian). AB was calibrated using a purified polysaccharide GX (Passow and Alldredge,
150 1995). TEP concentrations (μg gum xanthan [GX] equivalents L^{-1}) were measured according
151 to (Passow and Alldredge, 1995). Total TEP content in the mesocosms was calculated by
152 integrating the weighted average of the TEP concentrations per depth and multiplying by the
153 specific volume of each mesocosm. To estimate the role of TEP in C cycling, total amount of
154 TEP-C was calculated for each mesocosm, using the volumetric TEP concentrations at each
155 depth, the specific volume per mesocosm, and the conversion of GX equivalents to carbon
156 applying the revised factor of 0.63 based on empirical experiments from both natural samples
157 from different oceanic areas and phytoplankton cultures (Engel, 2004).

158 **2.3 TOC, POC, DOC**

159 Samples for total organic carbon (TOC) concentrations were collected in duplicate from
160 6 m in each mesocosm and in lagoon waters in precombusted sealed glassware flasks,
161 acidified with H₂PO₄ and stored in the dark at 4 °C until analysis. Samples were analyzed on a
162 Shimadzu TOCV analyzer with a typical precision of 2 μmol L⁻¹. Samples for particulate
163 organic carbon (POC) concentrations were collected by filtering 2.3 L of seawater through a
164 precombusted GF/F filter (450 °C for 4 h), combusted and analyzed on an EA 2400 CHN
165 analyzer. Dissolved organic carbon (DOC) concentrations were calculated as the difference
166 between TOC and POC concentrations. Fully detailed methodologies and data are available in
167 Berthelot et al. (2015).

168 **2.4 Dissolved inorganic phosphorus (DIP) and alkaline phosphatase activity**
169 **(APA)**

170 The determination of DIP concentrations are detailed in Berthelot et al. (2015). Samples
171 for DIP were collected from each of the three depths in M1, M2 and M3 and lagoon waters
172 (O) in 40 mL glass bottles, and stored in -20 °C until analysis. DIP concentration was
173 determined using a segmented flow analyzer according to (Aminot and K  rouel, 2007). The
174 alkaline phosphatase activity (APA) was measured from the same depths and sites using the
175 analog substrate methylumbelliferone phosphate (MUF-P, 1 μM final concentration;
176 SIGMA), (Hoppe, 1983). Full details of the measurements and analyses are described in Van
177 Wambeke et al. (This issue).

178 **2.5 Chlorophyll a (Chl a), Primary production (PP) and DIP turnover time**

179 Chlorophyll a (Chl a) concentrations were determined by fluorimetry and the detailed
180 methodologies also for primary production are described in Berthelot et al. (2015). Briefly,
181 primary production (PP) rates and DIP turnover time (T_{DIP}, i.e., the ratio of PO₄⁻³
182 concentration and uptake) were measured using the ¹⁴C/³³P dual labeling method (Duhamel et
183 al., 2006). 60 mL bottles were amended with ¹⁴C and ³³P and incubated for 3 to 4 h. This was
184 followed by the addition of 50 μL of KH₂PO₄ solution (10 mmol L⁻¹) to stop ³³P assimilation.
185 Samples were kept in the dark to stop ¹⁴C uptake. Samples were filtered on 0.2 μm
186 polycarbonate membrane filters, and counts were done using a Packard Tri-Carb® 2100TR
187 scintillation counter. PP and T_{DIP} were calculated according to (Moutin et al., 2002).

188 **2.6 Bacterial production (BP)**

189 Heterotrophic bacterial production (BP) was estimated using the ^3H -leucine
190 incorporation technique (Kirchman, 1993), adapted to the centrifuge method (Smith and
191 Azam, 1992). The complete methodology including enumeration of heterotrophic bacterial
192 abundances (BA) by flow cytometry is detailed in Van Wambeke et al. (This issue).

193 **2.7 N₂ fixation, diazotrophic abundance and growth rates**

194 N₂ fixation rates were determined daily on ambient waters from mesocosms and the
195 lagoon. Samples were spiked with 99% $^{15}\text{N}_2$ -enriched seawater, incubated in-situ under
196 ambient light and seawater temperatures as detailed in Berthelot et al. (2015) and (Bonnet et
197 al., This issue-a).

198 Data and protocols of sampling for diazotrophic abundance and calculation of their
199 respective growth rates are detailed fully in Turk-Kubo et al. (2015). Briefly, samples (from 6
200 m only) were collected every other day from the mesocosms, and from the lagoon waters.
201 DNA was extracted and nine diazotrophic phylotypes were identified using quantitative PCR
202 (qPCR). The targeted diazotrophs were two unicellular diazotrophic symbionts of different
203 *Braarudosphaera bigelowii* strains, UCYN-A1, UCYN-A2; free-living unicellular diazotroph
204 cyanobacterial phylotypes UCYN-B (*Crocospaera* sp.), and UCYN-C (*Cyanothece* sp. and
205 relatives); *Trichodesmium* spp.; and three diatom-diazotroph associations (DDAs), *Richelia*
206 associated with *Rhizosolenia* (Het-1), *Richelia* associated with *Hemiaulus* (Het-2), *Calothrix*
207 associated with *Chaetoceros* (Het-3), and a widespread gamma-proteobacterial phylotype γ -
208 24774A11. Abundances are reported as *nifH* copies L⁻¹ as the number of *nifH* copies per
209 genome in these diazotrophs are uncertain. Growth and mortality rates were calculated for
210 individual diazotrophs inside the mesocosms when abundances were higher than the limit of
211 quantification (LOQ) for two consecutive sampling days as detailed in Turk-Kubo et al.
212 (2015).

213 **2.8 Microscopic Analyses**

214 Detailed method for sampling for microscopic analyses is described in Bonnet et al.
215 (This issue). Phytoplankton were visualized using a Zeiss Axioplan (Zeiss, Jena, 6 Germany)
216 epifluorescence microscope fitted with a green (510-560 nm) excitation filter, which targeted
217 the *Richelia* and the UCYN phycoerythrin-rich cells. The diatom-diazotroph association
218 *Rhizosolenia-Richelia* were imaged in bright-field.

219 **2.9 Statistical analyses**

220 Statistical analyses were carried out with XLSTAT, a Microsoft Office Excel based
221 software. A Pearson correlation coefficient test was applied to examine the association
222 between two variables (TEP versus physical, chemical, or physiological variable) after linear
223 regressions or log-transformation of the data. The non-parametric Kruskal–Wallis one-way
224 analysis of variance was applied to compare between TEP dynamics from each of the
225 different phases. A confidence level of 95% (α - 0.05) was used.

226

227 **3 Results and Discussion**

228 **3.1 General context and spatial and temporal dynamics of TEP**

229 The VAHINE experiment was designed to induce and follow diazotrophic blooms and
230 their fate within an oligotrophic environment (Bonnet et al., This issue-b). Our specific
231 objectives of investigating TEP dynamics were thus examined within the general context and
232 aims of the large experiment. The first stage of the experiment involved the enclosure of the
233 lagoon waters and 3 days of equilibration of the system (P0 – pre-fertilization days 2-4). At
234 this initial stage the total Chl *a* concentrations averaged around $0.2 \mu\text{g L}^{-1}$ in the lagoon water
235 and in the mesocosms and the phytoplankton consisted of diverse representatives from the
236 cyanobacteria (*Prochlorococcus*, *Synechococcus*, diatoms such as *Pseudosolenia calcar-avis*,
237 and dinoflagellates) (Leblanc et al., This issue). During P0, the most abundant members of the
238 diazotrophic community in the lagoon waters were *Richelia-Rhizosolenia* (Het-1), the
239 unicellular UCYN-A1, UCYN-A2, UCYN-C, and the filamentous *Trichodesmium* (Turk-
240 Kubo et al., 2015).

241 Fertilization of the mesocosms with DIP on day 4 stimulated a two-stage response by
242 the diazotrophic community that was further reflected by many of the measured chemical and
243 biological parameters (Berthelot et al., 2015; Turk-Kubo et al., 2015; Bonnet et al., This
244 issue-a; Bonnet et al., This issue-b). After fertilization, from day 5 through day 14 (P1),
245 excluding a significant increase in N_2 fixation rates, the functional community-wide
246 biological responses (Chl *a*, PP, BP, BA) remained relatively low and similar to the values for
247 P0 and for P1 in the outside lagoon waters (Berthelot et al., 2015; Leblanc et al., This issue;
248 Van Wambeke et al., This issue). The autotrophic community during P1 was comprised of
249 picophytoplankton such as *Prochlorococcus*, and *Synechococcus*, micro and
250 nanophytoplankton including dinoflagellates, and a diverse diatom community (*Chaetoceros*,

251 *Leptocylindrus*, *Cerataulina*, *Guinardia*, and *Hemiaulus*), (Leblanc et al., This issue). Diatom-
252 diazotroph associations (DDAs), predominantly *Richelia-Rhizosolenia* (Het-1) dominated the
253 diazotroph community in the mesocosms (Turk-Kubo et al., 2015) although it still only
254 contributed from 2% to ~8% of the total diatom biomass in P0 and P1 respectively (Leblanc
255 et al., This issue). These DDAs were succeeded during the last 9 days (day 15 to 23 termed
256 P2) by a large bloom of unicellular diazotrophs characterized predominantly as UCYN-C
257 (Turk-Kubo et al., 2015).

258 The final stage of the experiment (P2, days 15-23) was characterized by significantly
259 enhanced values for many biological parameters including N₂ fixation rates, Chl *a*, PP, BA,
260 BP, and particulate organic carbon and nitrogen compared to their respective average values
261 in P1 (Leblanc et al., This issue; Van Wambeke et al., This issue; Bonnet et al., This issue-a).
262 In all three mesocosms, a significant bloom of UCYN-C developed (day 11 – M1, day 13-M2,
263 day 15-M3) and remained dominant representatives of the diazotroph community until day
264 23(Turk-Kubo 2015). The ambient autotrophic community responded to the input of new N,
265 and the transfer of diazotroph derived N was demonstrated and seen in increasing abundance
266 of *Synechococcus* , pico-eukaryotes, and the non-diazotrophic diatoms *Navicula* and
267 *Chaetoceros* spp. (Leblanc et al., This issue; Van Wambeke et al., This issue; Bonnet et al.,
268 This issue-a). Thus the extremely high N₂ fixation rates during this experiment provided
269 sufficient new N to yield high Chl *a* concentrations (> 1.4 μg L⁻¹) and rates of PP (>2 μmol C
270 L⁻¹ d⁻¹)(Berthelot et al., 2015).

271 **3.1.1 Dynamics of TEP**

272 TEP concentrations for the entire experimental period ranged from ~22 to 1200 μg GX
273 L⁻¹. In each mesocosm and also in the lagoon waters (O), the TEP concentrations were similar
274 for the three sampled depths within the 15 m water-column with an overall average of 350 ±
275 180 μg GX L⁻¹ (Fig. S1). Temporally, TEP concentrations generally followed the three
276 distinct periods (P0, P1, P2) that coincided with the described experimental phases
277 characterized from the diazotrophic populations and the biogeochemical and biological
278 (production) parameters (Berthelot et al., 2015; Turk-Kubo et al., 2015; Leblanc et al., This
279 issue; Van Wambeke et al., This issue; Bonnet et al., This issue-a), (Fig. 1, Fig. S1).
280 Following the enclosure of the lagoon water in the mesocosms (day 2), TEP concentrations
281 increased from the lowest volumetric concentrations (averaging~ 50 μg GX L⁻¹) measured on
282 day 2 to reach maximum concentrations in each of the mesocosms (average of ~800 μg GX L⁻¹

283 ¹) on day 5, ~15 h after the mesocosms were fertilized with DIP (Fig. S1, Fig. 1a). From day 5
284 to day 14 (P1) average TEP content in M2 and M3 decreased slightly yet significantly ($p <$
285 0.05) with the major decline in all mesocosms measured from day 5 to 6 (Fig. 1, Fig. S1,
286 Table S1). From day 15 to 23 (P2) TEP concentrations in all mesocosms increased gradually
287 ($p < 0.05$) over the subsequent 9 days to reach $381 \pm 39 \mu\text{g GX L}^{-1}$ on day 23 (Fig. 1, Table
288 S1).

289 TEP concentrations in the lagoon waters were compared with those in the mesocosms.
290 These showed a similar pattern of increase in TEP during P0 and [P3-P2](#) while the gradual
291 decline in TEP concentrations during [P2-P1](#) was not statistically significant as observed in the
292 mesocosms (Fig. 1, Fig. S1). In the lagoon waters average TEP concentrations over the whole
293 experimental period day 2 to day 23 were $335 \pm 56 \mu\text{g GX L}^{-1}$. While temporal variations in
294 the three mesocosms were mostly statistically significant (Fig. 1, Table S1), the total TEP
295 content calculated for each mesocosm and for an equivalent volume of lagoon water based on
296 average mesocosm volume) did not differ significantly when we assessed all data obtained
297 during P1 and P2 (Fig. 2, $p > 0.05$, Kruskal–Wallis analyses of variance). The lack of
298 significant differences in total TEP content in the mesocosms throughout the experiment
299 could reflect the contrasting processes of formation and breakdown that together maintain a
300 relatively stable pool of available TEP.

301 Mechanical processes such as wave turbulence and tidal effects can influence TEP
302 formation and breakdown (and resulting content), (Stoderegger and Herndl, 1999; Passow,
303 2002). Our results indicate no obvious effects of these parameters on TEP content as these
304 were similar in the enclosed mesocosms and the outside lagoon (Fig. 1, Fig. 2). Moreover,
305 despite the initial increase in mesocosm TEP concentrations prior to DIP fertilization, and for
306 the first 15 h after fertilization, from day 5 to the end of the experiment, TEP concentrations
307 were similar for both DIP-fertilized mesocosms and the lagoon waters with low DIP
308 concentrations (Fig. 1, Fig. S1, Fig. 2). This implies that also DIP fertilization had no impact
309 on the resulting total TEP content in the mesocosms (Yet, see below section 3.2).

310 The relative uniformity and stability of TEP within the 15 m water column of both the
311 mesocosms and the lagoon waters reflects the homogeneity of the shallow lagoon system. The
312 variability between the three depths was statistically insignificant in many of the other
313 physical, chemical, and biological features of the mesocosms and the lagoon waters for
314 temperature, salinity, inorganic nutrients (N, P, Si), POC, PON, POP, DOC, Chl *a*, and
315 primary production and heterotrophic bacterial production (Berthelot et al., 2015; Van

316 Wambeke et al., This issue; Bonnet et al., This issue-b; Bonnet et al., This issue-a). In contrast
317 to some marine systems where TEP concentrations were correlated with the vertical
318 distribution of Chl *a* or POC (Passow, 2002; Engel, 2004; Ortega-Retuerta et al., 2009; Bar-
319 Zeev et al., 2009; Bar-Zeev et al., 2011), the results we obtained here showed no correlation
320 to the vertical (i.e. depth related) autotrophic signatures. Moreover, the similar TEP
321 concentrations at 1, 6, and 15 m do not support a sub-surface maxima in TEP concentrations,
322 stimulated by abiotic aggregation, at the sea-surface top layer as has been reported at 1 m
323 depth in different oceanic areas (Wurl et al., 2011). Abiotic processes of formation and
324 breakdown can be influential yet here we do not see a depth-correlated specific abiotic driver
325 and TEP were evenly distributed within the 15 m water column for all mesocosms (Fig. S1).

326 **3.2 DIP availability, APA, and TEP content.**

327 The average TEP concentrations we measured in the New Caledonian waters are
328 comparable to TEP concentrations reported from other marine environments such as the
329 eastern temperate-subarctic North Atlantic (Engel, 2004), the Ross Sea (Hong et al., 1997),
330 western Mediterranean – Gulf of Cadiz and the Straits of Gibraltar (García et al., 2002; Prieto
331 et al., 2006), the Gulf of Aqaba (northern Red Sea), (Bar-Zeev et al., 2009), in the northern
332 Adriatic Sea (Radić et al., 2005), and in the New Caledonia lagoon (Mari et al., 2007;
333 Rochelle-Newall et al., 2008).

334 While prediction as to the expected TEP concentrations with trophic or productive
335 status is difficult (Beauvais et al., 2003), decreasing availability of dissolved nutrients such as
336 nitrate and phosphate have been correlated with enriched TEP concentrations in both cultured
337 phytoplankton and natural marine systems (Engel et al., 2002; Brussaard et al., 2005; Urbani
338 et al., 2005; Bar-Zeev et al., 2011). In P-limited systems, low Chl *a* concentrations often
339 reflect the nutrient-stressed phytoplankton. As long as light and CO₂ are available, limitation
340 of essential nutrients results in an uncoupling between carbon fixation and growth during
341 which the excess photosynthate can be used to produce carbon-rich compounds including
342 TEP (Berman-Frank and Dubinsky, 1999; Mari et al., 2001; Rochelle-Newall et al., 2008).
343 Moreover, as DIP-availability declines, cells activate P-acquisition pathways and enzymes
344 such as APA to access P from other sources. Thus, and based on previous data (Bar-Zeev et
345 al., 2011), we hypothesized that TEP content would be negatively correlated with autotrophic
346 biomass (Chl *a*) and PP and positively correlated with APA.

347 Mesocosm fertilization on the evening of day 4 enriched the system with ten-fold
348 higher DIP concentrations that were available for microbial utilization throughout the
349 following 8 – 10 days (Berthelot et al., 2015; Van Wambeke et al., This issue; Leblanc et al.,
350 This issue; Bonnet et al., This issue-b). Thus, when DIP concentrations were relatively
351 sufficient during P1, no statistically significant relationship was observed between TEP and
352 POP, DIP, T_{DIP} , Chl *a*, or PP (Table S2). This situation changed with the declining availability
353 of DIP and the shift in the response of the system during P2 from day 15 to 23. During P2
354 high TEP concentrations were associated with decreasing DIP for each of the mesocosms with
355 an overall negative correlation ($R^2 = 0.23$, $n = 23$, $p = 0.02$), (Fig. 3a). A similar negative
356 trend was obtained between TEP and the turnover time of DIP (T_{DIP}) which can indicate DIP
357 limitation ($R^2=0.28$ $n= 26$, $p= 0.006$), (Fig. 3b).

358 In the South West Pacific, the critical DIP turnover time (T_{DIP}) required for single
359 filaments of *Trichodesmium* to grow is 2 d (Moutin et al., 2005). Here T_{DIP} values lower than
360 1 d, indicative of a strong DIP deficiency, were reached on day 14 in M1, day 19 for M2, and
361 on day 21 for M3 with the average T_{DIP} values during P2 significantly different in each
362 mesocosm, T_{DIP} of 0.5, 1.8, 3.9 d for M1, M2, M3, respectively (Berthelot et al., 2015). The
363 deficiency in DIP was reflected in the subsequent APA which increased rapidly in both M1
364 and M2 from day 18 (average for M1 and M2 during P2 $\sim 8 \pm 6$ nmol MUF $l^{-1} h^{-1}$) and after
365 day 21 in M3 illustrating a biological response of the microbial community to P stress (Van
366 Wambeke et al., This issue). We did not specifically measure TEP production by autotrophic
367 or heterotrophic plankton. Yet, the significant (although indirect relationship) negative
368 correlation of TEP with DIP concentrations and T_{DIP} (Fig. 3a-b) suggests that microbial
369 responses to decreased DIP availability resulted from either 1) an increase in TEP synthesis
370 through higher polysaccharide production rather than biomass which requires higher nutrients
371 (Berman-Frank and Dubinsky 1999, (Wood and Van Valen, 1990), or 2) nutrient limitation
372 inducing greater breakdown of biomass and POM (maybe via programmed cell death) and
373 subsequent abiotic formation of TEP. We obtained a significant semi-logarithmic relationship
374 between TEP and APA ($R^2 = 0.33$ $n= 25$, $p = 0.002$), (Fig. 3c) which implies active TEP
375 formation when DIP concentrations are reduced and APA increases until a saturating point
376 whereby any further increases in APA do not appear to impact TEP concentrations (Fig. 3c).
377 This relationship may not always be valid as APA in the lagoon waters was consistently
378 higher at 1 m than APA measured at 6 and 12 m depths (Van Wambeke et al., This issue), yet
379 TEP concentrations were uniform at all depths (Fig. S1).

380 3.3 TEP and carbon pools

381 The size range of TEP spans a range of particles from 0.45 to 300 μm (Alldredge et al.,
382 1993; Bar-Zeev et al., 2015). TEP precursors (0.05 to 0.45 μm size) are formed and broken
383 down in the DOC pool and thus essentially “TEP establish a bridge between DOM (including
384 DOC) and the POM pool” (Engel, 2004). Our data shows a generally stable contribution of
385 TEP to the TOC pool. Excluding day 5, where TEP-C comprised $56.5 \pm 8\%$ of TOC, the %
386 TEP-C was $28.9 \pm 9.3\%$ and $27.0 \pm 7.2\%$ of the TOC in all mesocosms and in the lagoon
387 waters, respectively (Fig. 4a-b).

388 TEP concentrations can be directly and positively correlated with POC (Engel, 2004)
389 and with DOC (Ortega-Retuerta et al., 2009). Yet, TEP concentrations can also be negatively
390 related to POC indicative of low TEP production when POC concentrations are high (Bar-
391 Zeev et al., 2011). In the mesocosms, a significant positive correlation between TEP
392 concentrations and TOC was obtained for all three mesocosms only during P2 ($R^2 = 0.75$,
393 0.73, 0.58 and $p < 0.05$ for M1, M2, M3 respectively), (Fig. 4c, Table S2). This period
394 coincided with the largest gain in total autotrophic and heterotrophic biomass and elevated N_2
395 fixation, PP, and BP rates (Berthelot et al., 2015; Van Wambeke et al., This issue; Bonnet et
396 al., This issue-a).

397 Although TEP was significantly and positively correlated with TOC in the mesocosms
398 during P2, this was not the case with either POC or DOC in any mesocosm for either P1 or P2
399 (Table 1). The absence of any significant correlation between TEP and POC was surprising as
400 TEP are part of the POC pool comprising 40 – 60% of the particulate combined carbohydrates
401 in POC (Engel, 2004; Engel et al., 2012). Furthermore, we did not obtain any significant
402 correlations of TEP and specific components of the dissolved organic matter such as
403 fluorescent dissolved organic matter (FDOM) or chromophoric dissolved organic matter
404 (CDOM) that was coupled to the dynamics of N_2 fixation in the mesocosms (Tedetti et al.,
405 This issue). The lack of significant correlation could partially reflect methodological issues. In
406 this experiment [and operationally according to published protocol (Passow and Alldredge
407 (1995)] TEP was measured on 0.45 μm filters – so that Alcian Blue stained particles included
408 particles $> 0.45 \mu\text{m}$ while POC was measured on GF/F (nominal pore size 0.7 μm). DOC is
409 typically considered for the $< 0.45 \mu\text{m}$ fraction (Thurman, 1985), although here no direct
410 measurements of DOC were made and DOC was obtained by subtracting POC from TOC.
411 Thus, DOC actually covered the $< 0.7 \mu\text{m}$ fraction. Our methodology therefore precluded
412 determination of the smaller TEP precursors that would contribute to the DOC and colloidal

413 pools (Villacorte et al., 2015). As such we probably overestimated TEP relative to POC and at
414 the same time underestimated TEP's contribution to the DOC pool (Bar-Zeev et al., 2009).
415 The lacking correspondence between TEP concentrations and the pools of POC and DOC
416 may also result from the uncoupling between formation and breakdown processes. Abiotic
417 processes, will modify relationships obtained between biotic TEP production and recycling
418 (Wurl et al., 2011). Thus, it is feasible that especially during P1 abiotic factors predominated
419 breaking down larger TEP particles into smaller TEP precursors that would be mobilized to
420 the DOC pool and would thus maintain a relatively stable TEP pool although we observed a
421 positive increase in TEP with increased blooms of DDAs (see below section 3.4.1).
422

423 **3.4 Production and utilization of TEP by primary and bacterial populations**

424 Typically TEP are formed by diverse algal and bacterial species (Mari and Burd 1998)
425 yet are utilized mostly by bacteria and grazers as a rich C source (Engel and Passow, 2001;
426 Azam and Malfatti, 2007; Bar-Zeev et al., 2015). Throughout this experiment (P1 and P2
427 stages) TEP was not significantly correlated to parameters related to autotrophic production
428 such as total Chl *a*, PP, non-diazotrophic diatom or cyanobacterial abundance, or the growth
429 and mortality rates of these populations (Table S2). Furthermore, during P1, no significant
430 relationship between TEP and BA (total or specific for high and low nucleic acid bacteria-
431 HNA or LNA respectively), BP, or division rates was noted in any of the mesocosms (Table
432 S2).

433 This changed during P2 when TEP was positively correlated to the increasing BP for all
434 three mesocosms (Pearson's correlation coefficient $R^2 = 0.63, 0.66, 0.69$ for M1, M2, and M3
435 respectively, $p < 0.05$), (Fig. 5). During P2, TEP was also strongly and positively correlated to
436 TOC, which significantly increased over this time period (Fig. 4c) due to the high production
437 rates of both photosynthetic and heterotrophic bacterial populations. However, although BP
438 and PP were positively associated during P2 (log-log transformation, Fig. 5 in Van Wambeke
439 et al. this issue), we found no direct correlation between TEP and PP for either linear (Table
440 S2) or log-transformed regression (not shown). This coupling between PP and BP, while a
441 concurrent association between TEP and BP occurred during P2, indicates TEP may have been
442 utilized by bacteria as a carbon source (Azam, 1998; Ziervogel et al., 2014) or provided a
443 suitable niche for aggregation and proliferation of heterotrophic bacteria.

444 **3.4.1 TEP and diazotrophic populations**

445 Overall N_2 fixation rates were not significantly correlated with TEP concentrations at
446 any time in the experiment (Table S2). Neither could we discern any direct evidence of TEP
447 providing a carbon source for heterotrophic diazotrophs as was found previously in the Gulf
448 of Aqaba where these organisms contributed greatly to the N_2 fixation rates (Rahav et al.,
449 2015). Indeed, no relationship was found between TEP concentrations and the abundance or
450 growth rates of the heterotrophic diazotrophs γ -24774A11 (Moisander et al., 2014). Although
451 these organisms were present throughout the experiment, and increased ~4 fold from day 9 to
452 15 especially in M3, they contributed only a small fraction to the total diazotrophic biomass
453 and N_2 fixation rates (Turk-Kubo et al., 2015).

454 Yet, discerning individual diazotroph populations revealed some species-specific
455 correspondence to TEP at certain periods during the experiment. For example, throughout the
456 experiment, net growth rates (i.e., based on differences of *nifH* copies L⁻¹ from day to day) of
457 the DDA *Richelia* (Het-1) associated with *Rhizosolenia* (Turk-Kubo et al., 2015) temporally
458 paralleled TEP concentrations in all mesocosms (Fig. 6a-c, Fig. 6e-f). During both P1 and P2
459 TEP concentrations were positively correlated with the net growth rates of Het-1 ($R^2=0.6$
460 $P=0.0001$, $n=19$ for all mesocosms (Fig. 6d). Although the DDAs dominated the diazotroph
461 community during P1 (primarily Het-1), their overall contribution to diatom biomass in the
462 mesocosm was low with only 2-8% of all diatom biomass (Leblanc et al., this issue). We did
463 not observe an overall relationship between TEP and total diatom biomass throughout
464 VAHINE although diatoms are well known for their TEP production especially when
465 nutrients are limiting and growth rates decline (Urbani et al., 2005; Fukao et al., 2010). Thus,
466 the positive association between TEP and the growth rates of Het-1 and not of the other
467 DDAs Het-2 and Het-3 is intriguing.

468 TEP was also associated with the growth rates of the unicellular UCYN-C diazotrophs
469 that bloomed during P2 and dominated the N₂ fixation rates or this period (Turk-Kubo et al.,
470 2015; Berthelot et al., 2015). During P2, UCYN-C net growth rates were positively correlated
471 with increasing TEP concentrations ($R^2= 0.65, 0.83, 0.88$ for M1, M2, M3 respectively, $p <$
472 0.05). Furthermore, UCYN-C formed large aggregates (100-500 μm) embedded in an organic
473 matrix possibly also comprised of TEP (Fig. 6g-h) and were predominantly responsible for
474 the enhanced export production ($22.4 \pm 5\%$ of exported POC), (Knapp et al., This issue;
475 Bonnet et al., This issue-a). High TEP content was obtained from sediment traps on days 15
476 and 16 (Fig. S1), corresponding to the height of the UCYN-C bloom in the mesocosms (Turk-
477 Kubo et al., 2015) and substantiating the role of TEP in facilitating export flux in the New
478 Caledonia lagoon (Mari et al., 2007).

479 ~~The diazotroph *Trichodesmium*, that can account for huge surface blooms in the New~~
480 ~~Caledonia lagoons (Rodier and Le Borgne, 2008; Rodier and Le Borgne, 2010), did not bloom~~
481 ~~or accumulate within the VAHINE mesocosms. Yet, on day 23 a dense surface accumulation~~
482 ~~was sighted on the surface of the lagoon waters (Spungin et al., This issue). Frequent~~
483 ~~sampling (every 2-4 h) over the subsequent two days yielded extremely high TEP~~
484 ~~concentrations ($> 800 \mu\text{g GX L}^{-1}$) from this rapidly declining biomass (Spungin et al., This~~
485 ~~issue) corresponding to previous work demonstrating high TEP concentrations in~~
486 ~~*Trichodesmium* from the New Caledonian lagoon that are undergoing autocatalytic~~

Field Code Changed

487 ~~programmed cell death (PCD), (Berman-Frank et al., 2004; Berman-Frank et al., 2007; Bar-~~
488 ~~Zeev et al., 2013). We showed that nutrient stressed, PCD induced *Trichodesmium* diverts~~
489 ~~available carbon from growth processes to produce large amounts of TEP (Berman-Frank and~~
490 ~~Dubinsky, 1999; Berman-Frank et al., 2007). The TEP produced combines with the decaying~~
491 ~~biomass to form large particles and aggregates that sink downwards (Bar-Zeev et al., 2013).~~
492 ~~Here, we could not quantify the flux of matter obtained after this ephemeral bloom crashed.~~
493 ~~Yet, it is reasonable to assume that the high TEP content and the > 90% decline in biomass~~
494 ~~over a 24 h period resulted in a large downward flux of TEP cellular debris aggregates as we~~
495 ~~had observed previously under laboratory experiments (Berman-Frank et al., 2007; Bar-Zeev~~
496 ~~et al., 2013).~~

497

498 **4 Conclusions**

499 Although physically separated from the surrounding lagoon, TEP formation and
500 breakdown was difficult to tease out in the VAHINE mesocosms where abiotic drivers
501 (turbulence, shear forces, chemical coagulation) and biotic processes (algal and bacterial
502 production and utilization) maintained an apparently constant pool of TEP within the TOC.
503 Total TEP content was generally stable throughout the experimental period of 23 days and
504 comprised ~28% of the TOC in the mesocosms and lagoon with uniform distribution in the
505 three sampled depths of the 15 m deep-water column.

506 TEP concentrations appeared to be impacted indirectly via changes in DIP availability
507 as it was biologically consumed in the mesocosms after fertilization. Thus, declining P
508 availability (low DIP, rapid T_{DIP} , and increased APA) was associated with higher TEP content
509 in all mesocosms. TEP concentrations were also positively associated with net growth rates of
510 two important diazotrophic groups: the DDA *Richelia-Rhizosolenia* (Fig. 6e-f), during P1 and
511 P2 (excluding days 21-23); and UCYN-C diazotrophs which bloomed during P2. High TEP
512 content in the sediment traps during the UCYN-C bloom indicates that TEP may have been
513 part of the organic matrix associated with the large aggregates of UCYN-C that were exported
514 to the sediment traps (Fig. 6g-h).

515 TEP may have also provided bacteria with a rich organic carbon source especially
516 during P2 when higher BP (stimulated by the higher PP) was positively correlated higher TEP
517 concentrations. High production of TEP also occurred in the lagoon water outside the
518 mesocosms on day 23 during the decline of a short-lived dense surface bloom of the
519 diazotrophic *Trichodesmium* (Spungin et al., This issue) . Our results emphasize the

520 complexities of the natural system and suggest that to understand the role of compounds such
521 as TEP, and their contribution to the DOC and POC pools, a wider perspective and
522 methodologies be undertaken to examine and characterize the different components of marine
523 gels (not only carbohydrate-based), (Verdugo, 2012; Bar-Zeev et al., 2015)

524

525 **Author contributions**

526 IBF conceived and designed the investigation of TEP dynamics within the VAHINE project.
527 TM, FVW, IBF, DS, and ER participated in the experiment and performed analyses of
528 samples and data, KTK analysed diazotrophic populations. IBF and DS wrote the manuscript
529 with contributions from all co-authors.

530

531 **Acknowledgements**

532 Many thanks to Sophie Bonnet who created, designed, and successfully executed the
533 VAHINE project .The participation of IBF, DS, and ER in the VAHINE experiment was
534 supported by the German-Israeli Research Foundation (GIF), project number 1133-13.8/2011
535 to IBF and through a collaborative grant to IBF and SB from MOST Israel and the High
536 Council for Science and Technology (HCST)-France. Funding for this research was provided
537 by the Agence Nationale de la Recherche (ANR starting grant VAHINE ANR-13-JS06-0002),
538 INSU-LEFE-CYBER program, GOPS, IRD and M.I.O The authors thank the captain and
539 crew of the R/V Alis; the SEOH divers service from the IRD research center of Noumea (E.
540 Folcher, B. Bourgeois and A. Renaud) and from the Observatoire Océanologique de
541 Villefranche-sur-mer (OOV, J.M. Grisoni), the technical service and support of the IRD
542 research center of Noumea. Thanks also to C. Guieu, F. Louis and J.M. Grisoni from OOV for
543 mesocosm design and deployment advice. Special thanks to H. Berthelot and all other
544 participants and PIs of the project for the joint efforts and for making their data available for
545 further analyses. This work is in partial fulfillment of the requirements for a PhD thesis for D.
546 Spungin at Bar Ilan University.

547

548

549 **References**

550

551 Alldredge, A. L., Passow, U., and Logan, B. E.: The abundance and significance of a class of
552 large, transparent organic particles in the ocean., *Deep Sea Research*, 40, 1131-1140, 1993.

553 Aminot, A., and K rouel, R.: Dosage automatique des nutriments dans les eaux marines:
554 m thodes en flux continu, Editions Quae, 2007.

555 Azam, F.: Microbial control of oceanic carbon flux: The plot thickens., *Science*, 280, 694-
556 696, 1998.

557 Azam, F., and Malfatti, F.: Microbial structuring of marine ecosystems, *Nature Reviews*
558 *Microbiology*, 5, 782-791, 2007.

559 Azetsu-Scott, K., and Passow, U.: Ascending marine particles: significance of transparent
560 exopolymer particles (TEP) in the upper ocean., *Limnol. & Oceanogr*, 49, 741-748, 2004.

561 Bar-Zeev, E., Berman-Frank, I., Liberman, B., Rahav, E., Passow, U., and Berman, T.:
562 Transparent exopolymer particles: Potential agents for organic fouling and biofilm formation
563 in desalination and water treatment plants, *Desalination and Water Treatment*, 3, 136-142,
564 2009.

565 Bar-Zeev, E., Berman, T., Rahav, E., Dishon, G., Herut, B., Kress, N., and Berman-Frank, I.:
566 Transparent exopolymer particle (TEP) dynamics in the eastern Mediterranean Sea, *Marine*
567 *Ecology-Progress Series*, 431, 107-118, 10.3354/meps09110, 2011.

568 Bar-Zeev, E., Avishay, I., Bidle, K. D., and Berman-Frank, I.: Programmed cell death in the
569 marine cyanobacterium *Trichodesmium* mediates carbon and nitrogen export, *The ISME*
570 *journal*, 7, 2340-2348, 2013.

571 Bar-Zeev, E., Passow, U., Romero-Vargas Castrill n, S., and Elimelech, M.: Transparent
572 exopolymer particles: from aquatic environments and engineered systems to membrane
573 biofouling, *Environmental science & technology*, 49, 691-707, 2015.

574 Beauvais, S., Pedrotti, M. L., Villa, E., and Lemee, R.: Transparent exopolymer particle
575 (TEP) dynamics in relation to trophic and hydrological conditions in the NW Mediterranean
576 Sea, *Marine Ecology-Progress Series*, 262, 97-109, 2003.

577 Benavides, M., Moisander, P., Berthelot, H., Dittmar T, rosso O, and Bonnet S: Mesopelagic
578 heterotrophic N₂ fixation related to organic matter composition in the Solomon and Bismarck
579 Seas (Southwest Pacific), *PLoS ONE*, in press.

580 Berman-Frank, I., and Dubinsky, Z.: Balanced growth in aquatic plants: Myth or reality?
581 Phytoplankton use the imbalance between carbon assimilation and biomass production to their
582 strategic advantage, *Bioscience*, 49, 29-37, 1999.

583 Berman-Frank, I., Bidle, K., Haramaty, L., and Falkowski, P.: The demise of the marine
584 cyanobacterium, *Trichodesmium* spp., via an autocatalyzed cell death pathway, *Limnol.*
585 *Oceanogr.*, 49, 997-1005, 2004.

586 Berman-Frank, I., Rosenberg, G., Levitan, O., Haramaty, L., and Mari, X.: Coupling between
587 autocatalytic cell death and transparent exopolymeric particle production in the marine
588 cyanobacterium *Trichodesmium*, *Environmental microbiology*, 9, 1415-1422, 2007.

589 Berthelot, H., Moutin, T., L'Helguen, S., Leblanc, K., H lias, S., Grosso, O., Leblond, N.,
590 Charri re, B., and Bonnet, S.: Dinitrogen fixation and dissolved organic nitrogen fueled
591 primary production and particulate export during the VAHINE mesocosm experiment (New
592 Caledonia lagoon), *Biogeosciences*, 12, 4099-4112, 10.5194/bg-12-4099-2015, 2015.

- 593 Biegala, I. C., and Raimbault, P.: High abundance of diazotrophic picocyanobacteria (< 3 μm)
594 in a Southwest Pacific coral lagoon, *Aquatic microbial ecology*, 51, 45-53, 2008.
- 595 Bonnet, S., Berthelot, H., Turk-Kubo, K., Fawcett, S., Rahav, E., Berman-Frank, I., and
596 l'Helguen, S.: Dynamics of N_2 fixation and fate of diazotroph-derived nitrogen during the
597 VAHINE mesocosm experiment (New Caledonia), This issue-a.
- 598 Bonnet, S., Helias, S., Rodier, M., Moutin, T., Grisoni, J. M., Louis, F., Folcher, E.,
599 Bourgeois, B., Boré, J. M., and Renaud, A.: Introduction to the project VAHINE: VAriability
600 of vertical and trophic transfer of diazotroph derived N in the South West Pacific, This issue-
601 b.
- 602 Brussaard, C., Mari, X., Van Bleijswijk, J., and Veldhuis, M.: A mesocosm study of
603 *Phaeocystis globosa* (Prymnesiophyceae) population dynamics: II. Significance for the
604 microbial community, *Harmful algae*, 4, 875-893, 2005.
- 605 Capone, D. G.: Marine nitrogen fixation: what's the fuss?, *Curr. Opin. Microbiol.*, 4, 341-348,
606 2001.
- 607 Duhamel, S., Zeman, F., and Moutin, T.: A dual-labeling method for the simultaneous
608 measurement of dissolved inorganic carbon and phosphate uptake by marine planktonic
609 species, *Limnology and Oceanography-Methods*, 4, 416-425, 2006.
- 610 Dupouy, C., Neveux, J., Subramaniam, A., Mulholland, M. R., Montoya, J. P., Campbell, L.,
611 Capone, D. G., and Carpenter, E. J.: Satellite captures *Trichodesmium* blooms in the
612 SouthWestern Tropical Pacific., *EOS, Trans American Geophysical Union.*, 81, 13-16, 2000.
- 613 Engel, A.: The role of transparent exopolymer particles (TEP) in the increase in apparent
614 particle stickiness (α) during the decline of a diatom bloom, *Journal of Plankton Research*, 22,
615 485-497, 2000.
- 616 Engel, A., and Passow, U.: Carbon and nitrogen content of transparent exopolymer particles
617 (TEP) in relation to their Alcian Blue adsorption, *Marine Ecology Progress Series*, 219, 1-10,
618 2001.
- 619 Engel, A., Goldthwait, S., Passow, U., and Alldredge, A.: Temporal decoupling of carbon and
620 nitrogen dynamics in a mesocosm diatom bloom, *Limnology and Oceanography*, 47, 3, 753-
621 761, 2002.
- 622 Engel, A.: Distribution of transparent exopolymer particles (TEP) in the northeast Atlantic
623 Ocean and their potential significance for aggregation processes, *Deep-Sea Research Part I-*
624 *Oceanographic Research Papers*, 51, 83-92, 2004.
- 625 Engel, A., Harlay, J., Piontek, J., and Chou, L.: Contribution of combined carbohydrates to
626 dissolved and particulate organic carbon after the spring bloom in the northern Bay of Biscay
627 (North-Eastern Atlantic Ocean), *Continental shelf research*, 45, 42-53, 2012.
- 628 Eppley, R. W., and Peterson, B. J.: Particulate organic-matter flux and planktonic new
629 production in the deep ocean, *Nature*, 282, 677-680, 10.1038/282677a0, 1979.
- 630 Falkowski, P. G.: Evolution of the nitrogen cycle and its influence on the biological
631 sequestration of CO_2 in the ocean, *Nature*, 387, 272-275, 1997.
- 632 Fukao, T., Kimoto, K., and Kotani, Y.: Production of transparent exopolymer particles by four
633 diatom species, *Fisheries science*, 76, 755-760, 2010.

- 634 García, C., Prieto, L., Vargas, M., Echevarría, F., Garcia-Lafuente, J., Ruiz, J., and Rubin, J.:
635 Hydrodynamics and the spatial distribution of plankton and TEP in the Gulf of Cadiz (SW
636 Iberian Peninsula), *Journal of Plankton Research*, 24, 817-833, 2002.
- 637 Garcia, N., Raimbault, P., and Sandroni, V.: Seasonal nitrogen fixation and primary
638 production in the Southwest Pacific: nanoplankton diazotrophy and transfer of nitrogen to
639 picoplankton organisms, *Marine Ecology-Progress Series*, 343, 25-33, 10.3354/meps06882,
640 2007.
- 641 Grossart, H. P., Simon, M., and Logan, B. E.: Formation of macroscopic organic aggregates
642 (lake snow) in a large lake: The significance of transparent exopolymer particles, plankton,
643 and zooplankton, *Limnology and Oceanography*, 42, 1651-1659, 1997.
- 644 Hong, Y., Smith, W. O., and White, A. M.: Studies on transparent exopolymer particles (TEP)
645 produced in the ross sea (antarctica) and by *Phaeocystis antarctica* (prymnesiophyceae),
646 *Journal of Phycology*, 33, 368-376, 1997.
- 647 Hoppe, H. G.: Significance of exoenzymatic activities in the ecology of brackish water:
648 measurements by means of methylumbelliferyl-substrates. , *Marine Ecology Progress Series*,
649 11, 299-308, 1983.
- 650 Kirchman, D.: Leucine incorporation as a measure of biomass production by heterotrophic
651 bacteria, *Handbook of methods in aquatic microbial ecology*. Lewis, 509-512, 1993.
- 652 Knapp, A. N., Fawcett, S. E., Martinez-Garcia, A., Haug, G., Leblond, N., Moutin, T., and
653 Sophie., B.: Nitrogen isotopic evidence for a shift from nitrate- to diazotroph-fueled export
654 production in VAHINE mesocosm experiments, This issue.
- 655 Leblanc, K., Cornet, V., Caffin, M., Rodier, M., Desnues, A., Berthelot, H., Heliou, J., and
656 Bonnet, S.: Phytoplankton community structure in the VAHINE mesocosm experiment, This
657 issue.
- 658 Logan, B. E., Passow, U., Alldredge, A. L., Grossart, H.-P., and Simon, M.: Rapid formation
659 and sedimentation of large aggregates is predictable from coagulation rates (half-lives) of
660 transparent exopolymer particles (TEP), *Deep Sea Research Part II: Topical Studies in
661 Oceanography*, 42, 203-214, 1995.
- 662 Mari, X., Beauvais, S., Lemée, R., and Pedrotti, M. L.: Non-Redfield C: N ratio of transparent
663 exopolymeric particles in the northwestern Mediterranean Sea, *Limnology and
664 Oceanography*, 46, 1831-1836, 2001.
- 665 Mari, X., Kerros, M. E., and Weinbauer, M. G.: Virus attachment to transparent exopolymeric
666 particles along trophic gradients in the southwestern lagoon of New Caledonia, *Applied and
667 Environmental Microbiology*, 73, 5245-5252, 10.1128/aem.00762-07, 2007.
- 668 Moisander, P. H., Serros, T., Paerl, R. W., Beinart, R. A., and Zehr, J. P.:
669 Gammaproteobacterial diazotrophs and *nifH* gene expression in surface waters of the South
670 Pacific Ocean, *The ISME journal*, 8, 1962-1973, 2014.
- 671 Moutin, T., Thingstad, T. F., Van Wambeke, F., Marie, D., Slawyk, G., Raimbault, P., and
672 Claustre, H.: Does competition for nanomolar phosphate supply explain the predominance of
673 the cyanobacterium *Synechococcus*?, *Limnology and Oceanography*, 47, 1562-1567, 2002.
- 674 Moutin, T., Van Den Broeck, N., Beker, B., Dupouy, C., Rimmelin, P., and Le Bouteiller, A.:
675 Phosphate availability controls *Trichodesmium* spp. biomass in the SW Pacific Ocean, *Marine
676 Ecology-Progress Series*, 297, 15-21, 2005.

- 677 Mulholland, M. R., and Capone, D. G.: The nitrogen physiology of the marine N₂-fixing
678 cyanobacteria *Trichodesmium* spp, Trends in plant science, 5, 148-153, 2000.
- 679 Ortega-Retuerta, E., Reche, I., Pulido-Villena, E., Agustí, S., and Duarte, C. M.: Uncoupled
680 distributions of transparent exopolymer particles (TEP) and dissolved carbohydrates in the
681 Southern Ocean, Marine chemistry, 115, 59-65, 2009.
- 682 Passow, U., and Alldredge, A. L.: A dye binding assay for the spectrophotometric
683 measurement of transparent exopolymer particles (TEP), Limnol. & Oceanogr, 40, 1326-
684 1335, 1995.
- 685 Passow, U.: Transparent exopolymer particles (TEP) in aquatic environments, Progress in
686 Oceanography, 55, 287-333, 2002.
- 687 Postgate, J. R., and Eady, R. R.: The evolution of biological nitrogen fixation, in: Nitrogen
688 Fixation: One Hundred Years After, edited by: Bothe, H., DeBruijn, F. J., Newton, W.E,
689 Gustav Fischer, Stuttgart, 31-40., 1988.
- 690 Prieto, L., Navarro, G., Cozar, A., Echevarria, F., and García, C. M.: Distribution of TEP in
691 the euphotic and upper mesopelagic zones of the southern Iberian coasts, Deep Sea Research
692 Part II: Topical Studies in Oceanography, 53, 1314-1328, 2006.
- 693 Radić, T., Degobbi, D., Fuks, D., Radić, J., and Đakovac, T.: Seasonal cycle of transparent
694 exopolymer particles' formation in the northern Adriatic during years with (2000) and without
695 mucilage events (1999), Fresenius environmental bulletin, 14, 224-230, 2005.
- 696 Rahav, E., Bar-Zeev, E., Ohayion, S., Elifantz, H., Belkin, N., Herut, B., Mulholland, M. R.,
697 and Berman-Frank, I. R.: Dinitrogen fixation in aphotic oxygenated marine environments,
698 Frontiers in Microbiology, 4, 10.3389/fmicb.2013.00227, 2013.
- 699 Rahav, E., Herut, B., Mulholland, M. R., Belkin, N., Elifantz, H., and Berman-Frank, I.:
700 Heterotrophic and autotrophic contribution to dinitrogen fixation in the Gulf of Aqaba,
701 Marine Ecology Progress Series, 522, 67-77, 2015.
- 702 Rochelle-Newall, E., Torreton, J.-P., Mari, X., and Pringault, O.: Phytoplankton-
703 bacterioplankton coupling in a subtropical South Pacific coral reef lagoon, Aquatic Microbial
704 Ecology, 50, 221, 2008.
- 705 Rodier, M., and Le Borgne, R.: Population dynamics and environmental conditions affecting
706 *Trichodesmium* spp. (filamentous cyanobacteria) blooms in the south-west lagoon of New
707 Caledonia, Journal of Experimental Marine Biology and Ecology, 358, 20-32,
708 10.1016/j.jembe.2008.01.016, 2008.
- 709 Rodier, M., and Le Borgne, R.: Population and trophic dynamics of *Trichodesmium thiebautii*
710 in the SE lagoon of New Caledonia. Comparison with *T. erythraeum* in the SW lagoon,
711 Marine Pollution Bulletin, 61(7-12), 349-359, 10.1016/j.marpolbul.2010.06.018, 2010.
- 712 Smith, D. C., and Azam, F.: A simple, economic method for measuring bacterial protein
713 synthesis rates in seawater using ³H-leucine Mar. Microb. Food Webs 6, 107-114, 1992.
- 714 Spungin, D., Pfreundt, U., Berthelot, H., Bonnet, S., Al-Roumi, D., Natale, F., Hess, W. R.,
715 Bidle, K. D., and Berman-Frank, I.: Mechanisms of *Trichodesmium* bloom demise within the
716 New Caledonia Lagoon, This issue.
- 717 Stam, H., Stouthamer, A. H., and van Verseveld, H. W.: Hydrogen metabolism and energy
718 costs of nitrogen fixation, FEMS Microbiology Reviews, 46, 73-92, 1987.

719 Stoderegger, K. E., and Herndl, G. J.: Production of exopolymer particles by marine
720 bacterioplankton under contrasting turbulence conditions, *Marine Ecology Progress Series*,
721 189, 9-16, 1999.

722 Tedetti, M., Marie, L., Röttgers, R., Rodier, M., Van Wambeke, F., Helias, S., Caffin, M.,
723 Cornet-Barthaux, V., and Dupouy, C.: Evolution of dissolved and particulate chromophoric
724 materials during the VAHINE mesocosm experiment in the New Caledonian coral lagoon
725 (South West Pacific), This issue.

726 Thurman, E.: *Organic Geochemistry of Natural Waters*, Martinus Nijhoff/Dr W. Junk
727 Publishers, Dordrecht, 1985.

728 Turk-Kubo, K., Frank, I., Hogan, M., Desnues, A., Bonnet, S., and Zehr, J.: Diazotroph
729 community succession during the VAHINE mesocosms experiment (New Caledonia Lagoon),
730 *Biogeosciences Discussions*, 12, 2015.

731 Urbani, R., Magaletti, E., Sist, P., and Cicero, A. M.: Extracellular carbohydrates released by
732 the marine diatoms *Cylindrotheca closterium*, *Thalassiosira pseudonana* and *Skeletonema*
733 *costatum*: Effect of P-depletion and growth status, *Science of the Total Environment*, 353,
734 300-306, 2005.

735 Van Wambeke, F., Pfreundt, U., Barani, A., Berthelot, H., Moutin, T., Rodier, M., Hess.
736 W.R., and S, B.: Heterotrophic bacterial production and metabolic balance during the
737 VAHINE mesocosm experiment in the New Caledonia lagoon, *Biogeosciences Discussions*,
738 This issue.

739 Verdugo, P., and Santschi, P. H.: Polymer dynamics of DOC networks and gel formation in
740 seawater, *Deep Sea Research Part II: Topical Studies in Oceanography*, 57, 1486-1493, 2010.

741 Verdugo, P.: Marine microgels, *Annual review of marine science*, 4, 375-400, 2012.

742 Villacorte, L. O., Ekowati, Y., Calix-Ponce, H. N., Schippers, J. C., Amy, G. L., and
743 Kennedy, M. D.: Improved method for measuring transparent exopolymer particles (TEP) and
744 their precursors in fresh and saline water, *Water research*, 70, 300-312, 2015.

745 Wood, A., and Van Valen, L.: Paradox lost? On the release of energy-rich compounds by
746 phytoplankton, 1990.

747 Wurl, O., Miller, L., and Vagle, S.: Production and fate of transparent exopolymer particles in
748 the ocean, *Journal of Geophysical Research: Oceans* (1978–2012), 116, 2011.

749 Zehr, J. P., and Kudela, R. M.: Nitrogen Cycle of the Open Ocean: From Genes to
750 Ecosystems, in: *Annual Review of Marine Science*, Vol 3, *Annual Review of Marine Science*,
751 197-225, 2011.

752 Zhou, J., Mopper, K., and Passow, U.: The role of surface-active carbohydrates in the
753 formation of transparent exopolymer particles by bubble adsorption of seawater, *Limnology*
754 *and Oceanography*, 43, 1860-1871, 1998.

755 Ziervogel, K., D'souza, N., Sweet, J., Yan, B., and Passow, U.: Natural oil slicks fuel surface
756 water microbial activities in the northern Gulf of Mexico, *Frontiers in microbiology*, 5, 2014.

757

758

759 **Figure legends**

760 **Figure 1.** Temporal changes in transparent exopolymeric particle (TEP) concentrations (μg
761 GX L^{-1}) during the VAHINE mesocosm experiment. Data shown are from daily sampling of
762 three depths (1, 6, 12 m) in each mesocosm. Data was analyzed according to the characterized
763 phases of the experiment based on the diazotrophic communities that developed in the
764 mesocosms (Turk-Kubo et al., 2015) and biogeochemical characteristics (Bonnet et al., This
765 issue-a). **a.** Mesocosm 1 (M1) **b.** Mesocosm 2 (M2), **c.** Mesocosm 3 (M3), **d.** samples from
766 the lagoon waters outside of the mesocosms (O). Phases: P0= days 2-4, P1= days 5-14, P2=
767 days 15-23. Linear regressions (Pearson) of TEP for each of the phases are designated by a
768 solid line, only when significant. Pearson correlations coefficients and significant values ($p <$
769 0.05) are represented in bold in Table S1.

770 **Figure 2.** Total content of transparent exopolymeric particles (TEP) per mesocosm and in the
771 lagoon waters surrounding the mesocosms. The average amount in $\text{g GX mesocosm}^{-1}$ for the
772 two periods of the experiment after DIP fertilization was calculated from the total daily
773 amount based on concentrations measured at three depths and integrated for the specific
774 volume per mesocosm or for an equivalent volume of lagoon water. Averages are represented
775 in boxplots as a function of two different phases: P1 = days 5-14 and P2 = days 15-23. Red
776 (mesocosm 1 - M1), blue (mesocosm 2- M2), green (mesocosm - M3) and black (Outside
777 lagoon O). Straight lines within the boxes mark the median. No significant differences were
778 observed between the phases or between the three mesocosms and the outside lagoon
779 (Kruskal-Wallis non-parametric analysis of variance; $p > 0.05$).

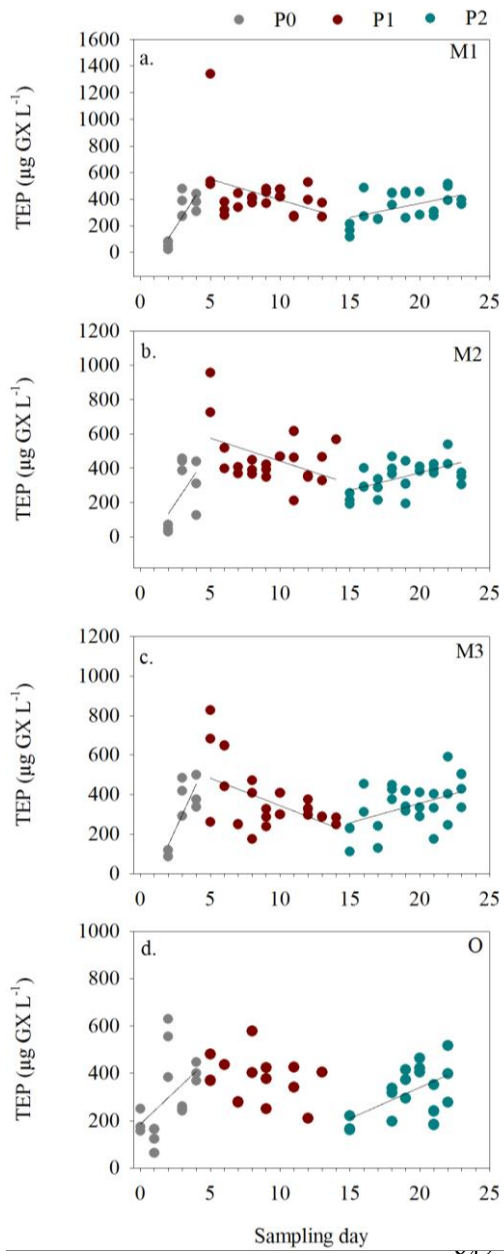
780 **Figure 3.** Relationships between the concentration of transparent exopolymeric particles
781 (TEP), ($\mu\text{g GX L}^{-1}$) and **a.** dissolved inorganic phosphorus DIP ($\mu\text{mol L}^{-1}$), **b.** turnover time of
782 DIP $-T_{\text{DIP}}$ (d) and **c.** alkaline phosphatase activity (APA), ($\text{nmol L}^{-1} \text{h}^{-1}$) in the three
783 mesocosms (M1-red; M2-blue; M3-green) during phase 2 (days 15-23). For a and b Pearson
784 linear regressions yielded an $R^2 = 0.54$, $n=23$ (TEP/DIP) and an $R^2=0.52$, $n=26$ (TEP/ T_{DIP}),
785 and for c. Log-transformed ($\log(\text{TEP}) / \log(\text{APA})$) with $R^2 0.68$, $n=25$. All correlations were
786 significant ($p < 0.05$). Error bars represent ± 1 standard deviation.

787 **Figure 4. a.** Temporal dynamics of TEP carbon concentrations (TEP-C, μM) in relationship
788 to the average total organic carbon (TOC), ($\mu\text{g L}^{-1}$), (thin black line) in the mesocosms (M1-
789 red dots, M2-blue dots, M3-green dots, and black dots- Outside waters (O)). Black solid line
790 designates TEP-C averaged for the three mesocosms (thick black line). TEP-C was measured

791 from 6 m depths and calculated according to Engel (2000). **b.** Temporal changes in the
792 percent of TEP-C from TOC (%) in mesocosms (green dots), and %TEP-C in the lagoon
793 waters (Out), (black dots). **c.** Relationship between TEP concentrations ($\mu\text{g GX L}^{-1}$) and TOC
794 ($\mu\text{mole L}^{-1}$), during phase 2 (days 15-23) for Mesocosm 1 (M1, red dots), Mesocosm 2 (M2,
795 blue dots), Mesocosm 3 (M3, green dots). Significant correlations were observed (Pearson)
796 for all mesocosms. $R^2 = 0.75$ - M1, 0.73 -M2, and 0.58 -M3 respectively, $n=7-8$, $p < 0.05$.
797 All statistics are detailed in Table S2. ($p=0.05$, $n= 7-8$). Error bars represent ± 1 standard
798 deviation.

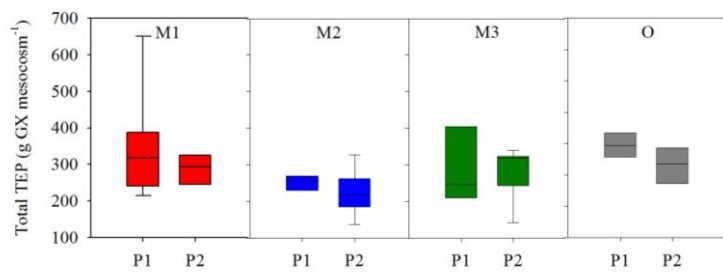
799 **Figure 5.** Relationship between heterotrophic bacterial production (BP), ($\text{ng C L}^{-1} \text{h}^{-1}$) and
800 TEP concentrations ($\mu\text{g GX L}^{-1}$) during phase 2 (days 15-23) when BP increased following
801 the enhanced PP (Van Wambeke et al., This issue), for Mesocosm 1 (M1, red dots),
802 Mesocosm 2 (M2, blue dots), Mesocosm 3 (M3, green dots). Pearson's linear regressions
803 yielded $R^2 = 0.57$ for M1, 0.42 for M2, and 0.56 for M3 respectively. Significant correlations
804 were observed for all mesocosms and are detailed in Table S2. Error bars represent ± 1
805 standard deviation.

806 **Figure 6.** Temporal changes in TEP concentrations and Het-1 net growth rates (d^{-1}), (gray
807 triangles) for **a.** Mesocosm 1 (M1) **b.** Mesocosm 2 (M2), **c.** Mesocosm 3 (M3). TEP
808 concentrations were averaged from the three depths sampled per mesocosm (green circles).
809 Het-1 net growth rates were calculated based on changes of *nifH* copies L^{-1} (Turk-Kubo et al.,
810 2015) measured every other day. **d.** Relationship between TEP concentrations ($\mu\text{g GX L}^{-1}$)
811 and
812 Het-1 growth rate (d^{-1}) for all three mesocosms. Significant correlations were observed
813 (Pearson) from all mesocosms together. $R^2 = 0.60$, $p=0.0001$, $n=19$. Error bars represent ± 1
814 standard deviation. **e-f.** Epifluorescent microscopical images of the diatom-diazotroph
815 association *Richelia-Rhizosolenia* identified by Het-1 abundance. Images by V. Cornet-
816 Barthaux. **g-h.** the diazotroph UCYN-C which bloomed and formed large aggregates
817 (comprised also of TEP) that enhanced vertical flux and export production during P2. Images
818 by S. Bonnet.
819



846 **Figure 2**

847



853

854

855

856

857

858

859

860

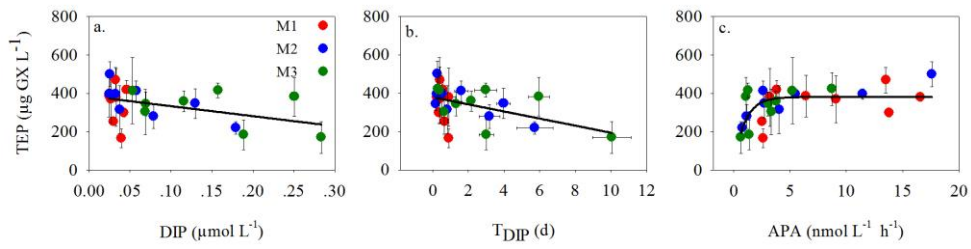
861

862

863 **Figure 3**

864

865



866

867

868

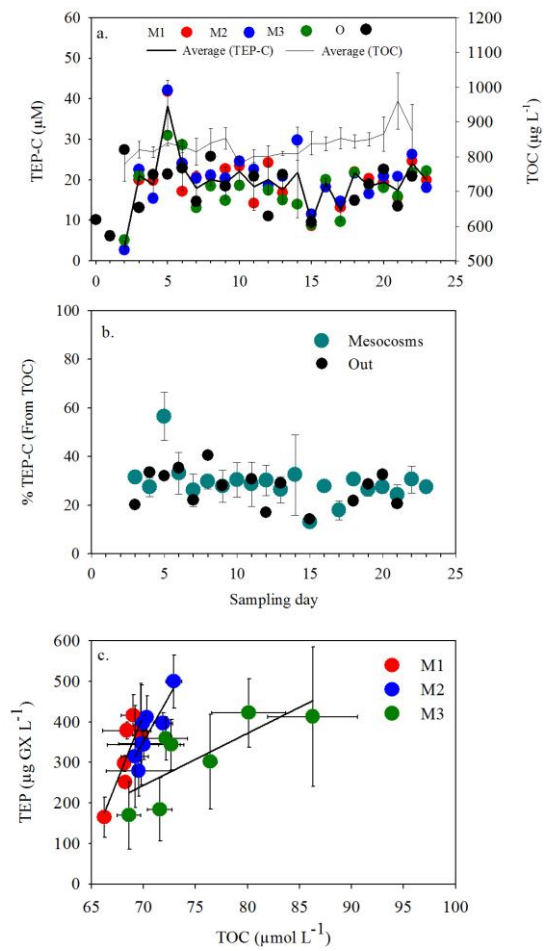
869

870

871 **Figure 4**

872

873



891

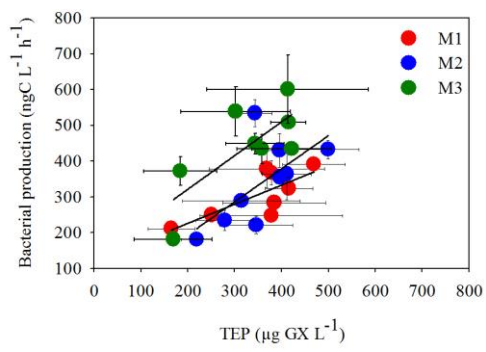
892

893

894 **Figure 5**

895

896



897

898

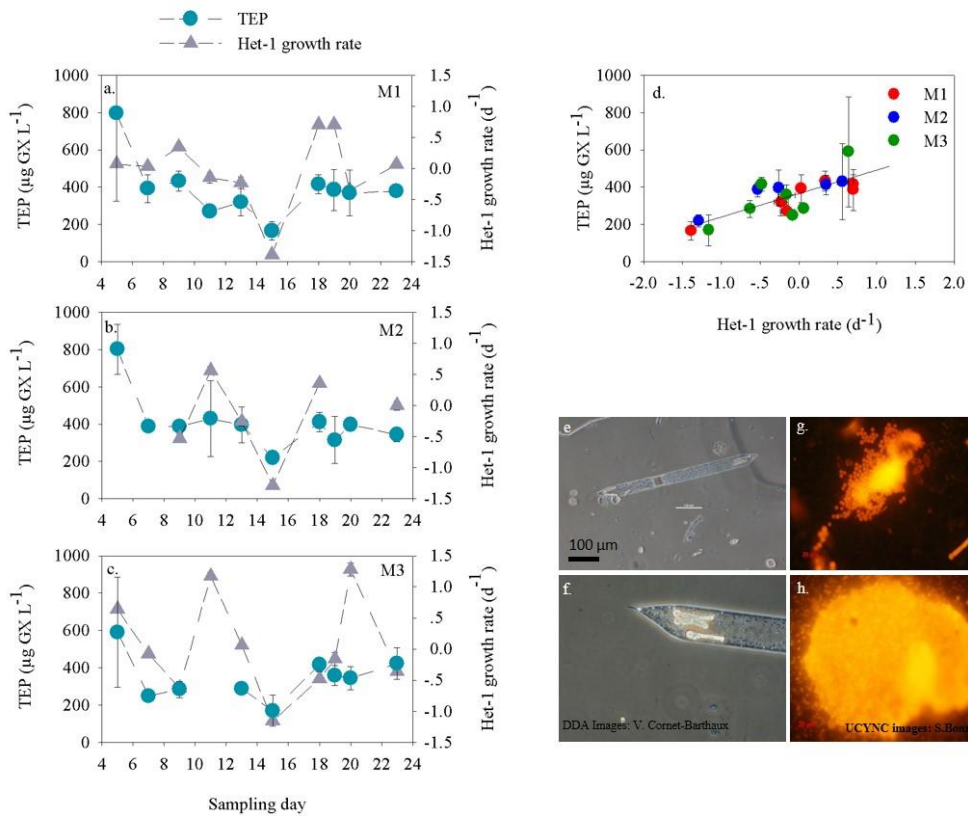
899

900

901 **Figure 6**

902

903



904

905

906

907

908

909